Transaction of the Society of Mechanical Engineers, Vol. 9, No. 4, pp. 487~496, 1985.

<Original>

Vibration Analysis of Rotating Thin Shells of Revolution by Finite Element Method

Hyun Sil Kim* and Young Whan Lee*

(Received February 28, 1985)

유한요소법에 의한 회전하는 얇은 축대칭 셸의 진동에 관한 연구

김 현 실·이 영 환

Key Words: Vibration(진동), Shell(셸), FEM(유한요소법), Coriolis(코리올리스), Sturm(스텀)

초 록

회전하는 축대칭 얇은 셸구조물의 진동 특성을 유한요소법에 의하여 해석하였다. 2개의 절절을 가진 Conical Frustrum 형태의 축대칭 요소를 사용하였으며 원주방향의 변위는 Fourier Series로 분해하여서 방정식의 수를 상당히 줄일 수 있었다. Sanders-Koiter의 셸이론을 사용하였으며 진동모우드는 회전의 영향을 설명하기 위하여 대칭 및 비대칭 모우드를 모두 고려하였다.

Coriolis 행렬를 포함하는 운동방정식에서 고유 진동수를 계산하기 위해서 질량, 강성 및 Coriolis 행렬로 이루어지는 Hermitian 행렬의 Sturm Sequence Property를 이용하였으며, 좁은 밴드를 갖는 대형 행렬에 알맞는 Determinant Search 방법을 확장하여 고유진동수 및 벡터를 구하였다.

원통형 셸에 대하여 정지한 경우 계산한 고유진동수를 실험치 및 이론치와 비교한 결과 잘 일치됨을 알 수 있었다. 여러가지 회전 속도에 대해서 얻어진 고유진동수를 이론치와 비교한 결과 잘 일치됨을 알 수 있었으며 회전의 영향으로 traveling wave 진동의 현상이 나타남을 알 수 있었다.

1. Introduction

Thin shell structures are widely used in many industrial structures. Particularly, rotating shells have important application in certain rotor systems of gas turbine engines and machineries like centrifuges. While numerous references are available on the vibration of thin shells, few include the effect of rotation which causes the Coriolis terms. The existence of traveling waves in rotating systems is a well known phenomenon. Due to complicated governing equations of general thin shells, most vibration analysis have been concentrated on the cylindrical shells which have relatively simple geometry.

Macke[1] investigated traveling wave vibration of gas turbine engine shells which caused the fatigue crackes in forward compressor casings of aircraft jet engines. He obtained natural frequencies of rotating cylindrical shell having finite length and certain boundary conditions by assuming inextentional ring vibration and then introducing a correcting factor which is a function of geometry and circumferential wave number to satisfy the boundary conditions.

*Member, Korea Advanced Energy Research Institute

Srinivasan and Lauterbach[2] treated the vibration of long rotating cylindrical shells of which end conditions were neglected. They used the equations of motion including buckling terms due to axial, radial and torsional loading. Penzes[3] and Padoven[4] considered the anisotropic shell including the effects of rotation and prestresses. They obtained natural frequencies by using complex mode shapes. Penzes considered the cylindrical shell having arbitrary boundary conditions, while Padovan treated infinitely long cylindrical shell.

For rotating shells of revolution, Padovan[5] obtained the natural frequencies and buckling eigenvalues of prestressed shell by quasi-analytical finite element procedure. He included the effects of Coriolis forces, torque prestress and material anistropy.

In this paper, a vibration analysis of rotating thin shell having arbitrary shape of revolution by finite element method is presented. Sanders-Koiter[6] thin shell theory is used and circumferential variables are expanded into Fourier series so as to reduce the number of equations, which results in a considerable saving of computing time. To solve the equations of motion containing the Coriolis or gyroscopic matrix caused by rotation after conventional FEM formulation, the Sturm sequence property[7] of the Hermitian matrix consisted of mass matrix, stiffness matrix and Coriolis matrix is used. Eigenvalues are extracted from the solution routine where iteration of characteristic polynomial given by the determinant of Hermitian matrix and Rayleigh Quotient iteration for complex vectors are combined to calculate the eigenvalues of small banded-large order matrix most effectively.

For several non-rotating shells such as cylinder, cylinder-hemisphere structure and cooling tower, numerical results are compared with the results by various methods like FEM which used different elements or shape functions, FDM, numerical integration method, and analytical method. For rotating cylindrical shell, natural frequencies are computed and compared with theoretical results. In case of rotating, traveling waves are found.

2. Two Node Conical Element

An axi-symmetric thin shell is divided into

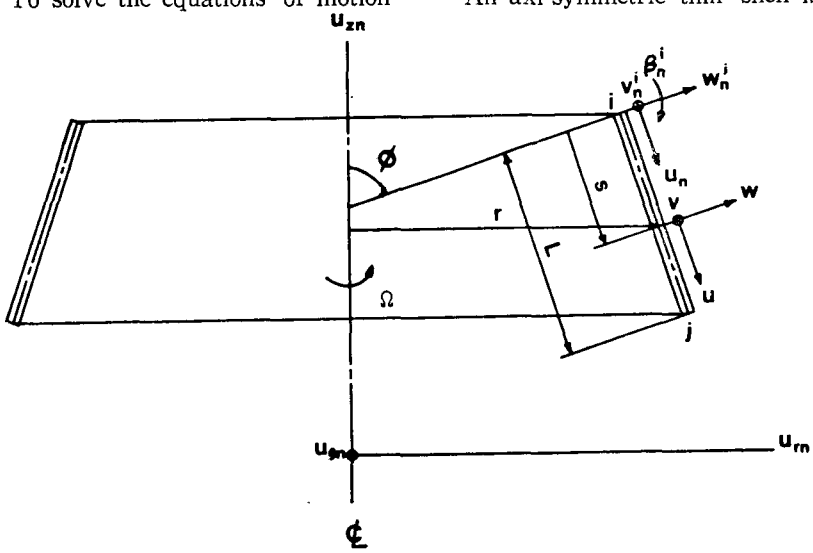

Fig. 1 Geometry and displacements of a two node conical element

the conical frustra as shown in Fig. 1. The displacements of mid-surface of the shell in local coordinates are u,v, and w, corresponding to meridional, circumferential and normal displacement respectively.

From Sanders-Koiter[6] shell theory, strain-displacement relations are given by

$$\epsilon_{ss}=\frac{\partial u}{\partial s} \tag{1a}$$

$$\epsilon_{\theta\theta}=\frac{\partial v}{r\,\partial\theta}+\frac{\cos\phi u}{r}+\frac{\sin\phi w}{r} \tag{1b}$$

$$\epsilon_{s\theta}=\frac{1}{2r}\left(\frac{\partial u}{\partial\theta}+r\frac{\partial v}{\partial s}-\cos\phi v\right) \tag{1c}$$

$$x_{ss}=-\frac{\partial^2 w}{\partial s^2} \tag{1d}$$

$$x_{\theta\theta}=\frac{1}{r^2}\left(-\frac{\partial^2 w}{\partial\theta^2}+\sin\phi\frac{\partial v}{\partial\theta}-r\cos\phi\frac{\partial w}{\partial s}\right) \tag{1e}$$

$$x_{s\theta}=\frac{1}{2r}\left[\left(-2\frac{\partial^2 w}{\partial s\partial\theta}+\frac{2}{r}\cos\phi\frac{\partial w}{\partial\theta}-\frac{2\cos\phi\sin\phi\, v}{r}\right)+\sin\phi\frac{\partial v}{\partial s}+\frac{1}{2r}\sin\phi\left(\cos\phi v+r\frac{\partial v}{\partial s}-\frac{\partial u}{\partial\theta}\right)\right] \tag{1f}$$

where $\epsilon_{ss}, \epsilon_{\theta\theta}$ and $\epsilon_{s\theta}$ are the meridional, circumferential and shear strains of the mid-surface, and $x_{ss}, x_{\theta\theta}$ and $x_{s\theta}$ are the changes of the curvatures, corresponding to each coordinate.

The displacements are expanded into Fourier series as follows:

$$\begin{pmatrix}u\\v\\w\end{pmatrix}=\sum_{n=0}^{\infty}\begin{bmatrix}\cos n\theta & 0 & 0 & \sin n\theta & 0 & 0\\ 0 & \sin n\theta & 0 & 0 & \cos n\theta & 0\\ 0 & 0 & \cos n\theta & 0 & 0 & \sin n\theta\end{bmatrix}\begin{pmatrix}u_n\\v_n\\w_n\\\hat{u}_n\\\hat{v}_n\\\hat{w}_n\end{pmatrix} \tag{2}$$

where the right-hand side displacements without hat and with hat denote the symmetric and anti-symmetric parts respectively. If rotating motion is not considered, anti-symmetric parts are dropped.

The nodal displacements at point i have eight components, $u^i{}_n$, $v^i{}_n$, $w^i{}_n$ and rotation $\beta^i{}_n$, and corresponding four anti-symmetric components. By using Hermitian polynomials of order 0 and 1, shape functions are determined from the conditions that slope and displacements should be continuous at nodal points. Then for the symmetric part one has

$$\begin{pmatrix}u_n\\v_n\\w_n\end{pmatrix}=\left[\begin{array}{cccc:cccc}1-s' & 0 & 0 & 0 & s' & 0 & 0 & 0\\ 0 & 1-s' & 0 & 0 & 0 & s' & 0 & 0\\ 0 & 0 & 1-3s'^2+2s'^3 & L(s'-2s'^3+s'^3) & 0 & 0 & 3s'^2-2s'^3 & L(-s'^2+s'^3)\end{array}\right]\begin{pmatrix}u^i{}_n\\v^i{}_n\\w^i{}_n\\\beta^i{}_n\\u^j{}_n\\v^j{}_n\\w^j{}_n\\\beta^j{}_n\end{pmatrix} \tag{3}$$

where $\beta^i{}_n=\frac{dw^i{}_n}{ds}$, $\beta^j{}_n=\frac{dw^j{}_n}{ds}$, and $s'=\frac{s}{L}$.

For anti-symmetric parts, the same functions are obtained. The nodal displacements at point i in local coordinates are transformed into the displacements in global coordinates as follows:

$$\begin{pmatrix}u^i{}_n\\v^i{}_n\\w^i{}_n\\\beta^i{}_n\end{pmatrix}=\begin{bmatrix}\cos\phi & 0 & -\sin\phi & 0\\ 0 & 1 & 0 & 0\\ \sin\phi & 0 & \cos\phi & 0\\ 0 & 0 & 0 & 1\end{bmatrix}\begin{pmatrix}u^i{}_{rn}\\u^i{}_{\theta n}\\u^i{}_{zn}\\\beta^i{}_n\end{pmatrix} \tag{4}$$

where $u^i{}_{rn}$, $u^i{}_{\theta n}$ and $u^i{}_{zn}$ are radial, circumferential and axial displacements in global coordinates respectively as shown in Fig. 1. The same expression is used for the displacements at node j and corresponding anti-symmetric parts.

3. Variational Formulation

The potential energy is given by the sum of strain energy and the work done by the hoop

stress due to centrifugal force. Strain energy is expressed as

$$U_s=\frac{Eh}{2(1-\nu^2)}\int_0^L\int_0^{2\pi}[\epsilon^2{}_{ss}+\epsilon^2{}_{\theta\theta}+2\nu\epsilon_{ss}\epsilon_{\theta\theta}+2(1-\nu)\epsilon^2{}_{s\theta}]rd\theta ds+\frac{Eh^3}{24(1-\nu^2)}\int_0^L\int_0^{2\pi}[x^2{}_{ss}+x^2{}_{\theta\theta}+2\nu x_{ss}x_{\theta\theta}+2(1-\nu)x^2{}_{s\theta}]\,rd\theta ds \quad (5)$$

Work done by the hoop stress due to the centrifugal force is given by

$$U_H=\int_0^L\int_0^{2\pi}N_\theta\epsilon^n{}_{\theta\theta}r\,d\theta ds \quad (6)$$

where N_θ is the hoop stress over thickness and $\epsilon^n{}_{\theta\theta}$ is the nonlinear circumferential strain. From Sanders-Koiter,

$$\epsilon^n{}_{\theta\theta}=\frac{1}{8r^2}\left(\cos\phi v+r\frac{\partial v}{\partial s}-\frac{\partial u}{\partial\theta}\right)^2+\frac{1}{2r^2}\left(\frac{\partial w}{\partial\theta}-\sin\phi v\right)^2 \quad (7)$$

Kinetic energy including rotating effect is expressed as

$$T=\frac{\rho h}{2}\int_0^L\int_0^{2\pi}[\dot u^2{}_z+(\dot u_r-u_\theta\Omega)^2+(\dot u_\theta+u_r\Omega)^2]\,rd\theta ds \quad (8)$$

where u_r, u_θ, and u_z are displacements in global coordinates and Ω is rotating speed.

Substiuting the strains in terms of nodal displacements in global coordinates into Eq. (5), (6), (7) and (8), and assembling energy expressions over all elements, one can obtain the equations of motion by applying the following variational principle:

$$\delta(U^t{}_s+U^t{}_H-T^t)=0 \quad (9)$$

where superscript small t means assembled form. By using the orthogonal properties of the harmonic functions, the equations of motion are separated for each circumferential wave number n and following expressions are obtained:

$$M_n\ddot R_n+C_n\dot R_n+K_nR_n=0 \quad (10)$$

where M_n is mass matrix, K_n is stiffness matrix, C_n is Coriolis or gyroscopic matrix, and R_n is displacement vector. M_n and K_n are real symmetric positive definite matrix, and C_n is a real skew-symmeric matrix. These matrices are highly banded matrices of order N. C_n is a function of Ω, rotating speed, such that $C_n=\Omega C_n'$. K_n is composed of three parts

$$K_n=K^e{}_n+K^H{}_n+K^c{}_n \quad (11)$$

where $K^e{}_n$ is the elastic stiffness matrix, $K^H{}_n$ is the geometrical stiffness matrix, function of Ω^2, and $K^c{}_n$ is the matrix incorporating centrifual force effect, function of Ω^2. If Ω is zero, Eq. (10) can be decoupled into two parts, symmetric and anti-symmetric parts as follows:

$$M_n{}^s\ddot R_n{}^s+K_n{}^sR_n{}^s=0 \quad (12a)$$

$$M_n{}^A\ddot R^A+K_n{}^AR_n{}^A=0 \quad (12b)$$

where superscript s and A mean symmetric and anti-symmetric parts respectively. Matrices in Eq. (12a) are exactly the same as corresponding matrices in Eq. (12b), and Eq. (12a) and Eq. (12b) become identical. The order of matrices is half as that of matrices in Eq. (10).

4. Eigenvalue Analysis

Eq. (10) can be rearranged as follows:

$$A_n\dot Q_n+B_nQ_n=0 \quad (13)$$

where

$$A_n=\begin{pmatrix}0 & M_n\\ M_n & C_n\end{pmatrix}\quad B_n=\begin{pmatrix}M_n & 0\\ 0 & K_n\end{pmatrix}$$

$$Q=\begin{pmatrix}\dot R_n\\ R_n\end{pmatrix} \quad (14)$$

Substituting $Q_n=X_ne^{-i\lambda t}$ into Eq. (13), one has

$$(B_n-i\lambda A_n)X_n=0 \quad (15a)$$

$$\text{or } (B_n-\lambda A^*{}_n)X_n=0 \quad (15b)$$

where X_n is complex eigenvector, λ is real eigenvalue, and $A^*{}_n=iA_n$. $A^*{}_n$ is a Hermitian matrix and B_n is a real symmetric positive definite matrix of order 2N. Then it follows that $(B_n-\lambda A^*{}_n)$ is a Hermitian matrix, and for a real value λ, the determiant of $(B_n-\lambda A^*{}_n)$ is real. λ is obtained from the following equation:

$$\det(B_n-\lambda A^*_n)=0 \tag{16}$$

From Gupta[8], it is known that $(B_n-\lambda A^*_n)$ has the Sturm sequence property, i.e., the number of solutions λ satisfying Eq. (16) between zero and some chosen vaule λ_c is equal to the number of reversals of sign between the diagonals of triangularized form of $(B_n-\lambda_c A^*_n)$. Based on this property, Gupta[8,9] made a subroutine where λ is isolated by using the Sturm sequence property of $(B_n-\lambda A^*_n)$, and then vector iteration is performed to calculate eignvalues and vectors. But in this procedure, the order of matrix is twice as that of Eq. (10), and this is a great disavantage.

Eq. (16) can be decomposed as follows:

$$\det(B_n-\lambda A^*_n)=\det(M_n)\ \det\ (D_n(\lambda)) \tag{17}$$

where

$$D_n(\lambda)=(K_n-\lambda^2 M_n-i\lambda C_n) \tag{18}$$

Since M_n is a real symmetric positive definite matrix, $\det(M_n)$ has a certain real value, not zero. So Eq. (16) is reduced as follows:

$$\det\ (D_n(\lambda))=0 \tag{19}$$

Wittrick[10] showed that $D_n(\lambda)$ has also the Sturm sequence property for a real λ where $D_n(\lambda)$ is a Hermitian matrix of order N. It can be easily shown that $-\lambda$ is also root and $\det\ (D_n(\lambda))$ is a function of λ^2 rather than of λ and in fact a polynomial of degree N in λ^2. Using these properties, a solution subroutine is established to calculate eigenvalues and eigenvectors. Its main idea is similar with thaf of the determinant search method[11], a widely used solution method for small banded real symmetric matric matrix, which is a combination of polynomial iteration and vector inverse iteration.

At present study, solution procedures are modified and expanded to cope with the polynomial of Hermitian matrix, $P(\lambda)=\det(D_n(\lambda))$, and the Rayleigh Quotient iteration for complex vectors as follows:

(1) λ is isolated by using the Sturm sequence property of the matrix $(K_n-\lambda^2 M_n-i\lambda C_n)$.

(2) A polynomial iteration is performed to obtain the appropriate initial eigenvalue for step(3) as follows:

$$\lambda_{l+1}=\lambda_l-\frac{P(\lambda_l)}{P(\lambda_l)-P(\lambda_{l-1})}\ (\lambda_l-\lambda_{l-1}) \tag{20}$$

$P(\lambda)$, determinant of $D_n(\lambda)$, is obtained by

$$P(\lambda)=\sum_{i=1}^{N} D_{ii} \tag{21}$$

D_{ii} is the diagonal of triangularized form of $D_n(\lambda)$. Iteration continues until following criteria is satisfied

$$\left|\frac{\lambda_{l+1}-\lambda_l}{\lambda_l}\right|<\epsilon \tag{22}$$

(3) More accurate eigenvalue and corresponding eigenvector are calculated by applying Rayleigh Quotient iteration by using λ_{l+1} given in step (2) as the starting λ_0.

$$\begin{pmatrix}\dot{y}_k\\ y_k\end{pmatrix}=\begin{pmatrix}0 & -iM_n\\ iM_n & iC_n\end{pmatrix}\begin{pmatrix}\dot{x}_k\\ x_k\end{pmatrix} \tag{23a}$$

$$(K_n-\lambda^2{}_k M_n-i\lambda_k C_n)\ x_{k+1}=i\lambda_k\dot{y}_k+y_k \tag{23b}$$

$$M_n\dot{x}_{k+1}=-i\lambda_k M_n x_{k+1}+\dot{y}_k \tag{23c}$$

$$\lambda_{k+1}=\lambda_k+\frac{\dot{x}^T{}_{k+1}\dot{y}_k+\bar{x}^T{}_{k+1}y_k}{\dot{x}^T{}_{k+1}\dot{y}_{k+1}+\bar{x}^T{}_{k+1}y_{k+1}} \tag{23d}$$

$$\dot{y}_{k+1}=\frac{\dot{y}_{k+1}}{(\dot{x}^T{}_{k+1}\dot{y}_{k+1}+\bar{x}^T{}_{k+1}y_{k+1})^{1/2}} \tag{23e}$$

$$y_{k+1}=\frac{y_{k+1}}{(\dot{x}^T{}_{k+1}y_{k+1}+\bar{x}^T{}_{k+1}y_{k+1})^{1/2}} \tag{23f}$$

Iteration continues until following criteria is satisfied

$$\left|\frac{\lambda_{k+1}-\lambda_k}{\lambda_k}\right|<\epsilon_1 \tag{24}$$

where $\dot{y}_k$, y_k, $\dot{x}_k$, and x_k are complex vectors and ϵ_1 is the required accuracy, much smaller than ϵ in Eq. (22). Eigenvalue λ can be obtained directly from step (2) using Eq. (22) with ϵ_1 instead of ϵ. But, generally this needs much computing time than presented procedures combined with the vector iteration.

After the first root is calculated, then the whole steps are repeated for next root until

required number of eigenvalues and eigenvectors are obtained.

5. Numerical Examples

Natural frequencies are calculated for various shells and compared with other results by finite element methods where different elements or shape functions were used, and by theoretical or experimental methods. For non-rotating shells, three comparisons are presented in Table 1, 2, and 3.

For a clamped-free cylindrical shell where some experimental and theoretial results are available, natural frequencies are given in Table 1 in which n is the circumferential wave number and m is the meridional mode number. Natural frequencies by present FEM analysis are in good agreement with theoretical results (ref. 12), while they show a little difference from experimental results (ref. 13) particularly when $n=2$ with maximum error of 7%.

As the second example, natural frequencies of a cylinder-hemisphere shell (Fig.2) are calculated ($L/D=0.5$, $h/D=0.01$, $E=1.0$, $\nu=0.2$, $\rho=1.0$, $L=100$). For $m=1$, the results are compared with the frequencies by various methods. The results denoted by FEM** in Table 2 were obtained by Galletly and Mistry (ref. 14) who used two kinds of elements, straight-sided element and curved element. They also carried out variational finite difference method (VFD). Natural frequencies by numerical integration method are also given in Table 2. All referred frequencies are taken from ref. (14), and results in Table 2 show a very good correspondence.

Thin shell in this example has dimensionless geometric characteristics and material properties. For actual structures having similar geometry to that in Fig. 2, natural frequencies may be calculated by multiplying the results in Table 2

Table 1 Natural frequencecies (Hz) of a clamped-free cylindrical shell of radius=63.5mm, length =502mm, thickness=1.63mm, $E=2.1\times10$ N^{11}/m^2, $\nu=0.28$, $\rho=7.8\times10^3 kg/m^3$

n		$m=1$	$m=2$	$m=3$	$m=4$
2	Expt.*	293.0	827.0	1894.8	—
	Theory**	319.5	1019.7	2398.9	3963.2
	FEM	316.2	948.6	2225.5	3716.5
3	Expt.	760.0	886.0	1371.0	2155.0
	Theory	769.8	930.4	1515.4	2428.3
	FEM	768.1	920.9	1484.6	2378.9
4	Expt.	1451.0	1503.0	1673.0	2045.0
	Theory	1465.8	1525.0	1730.3	2158.0
	FEM	1462.7	1521.0	1729.5	2168.6
5	Expt.	2336.0	2384.0	2480.0	2667.0
	Theory	2367.1	2409.2	2513.4	2722.6
	FEM	2362.3	2402.9	2512.1	2735.1
6	Expt.	3429.0	3476.0	3546.0	3667.0
	Theory	3470.3	3509.8	3586.6	3724.3
	FEM	3463.6	3499.9	3581.1	3728.3

* Experimental frequencies are taken from ref. (13).
** Theoretical frequencies are taken from ref. (12).

Table 2 Natural frequencies (Hz$\times 10^3$) of a cylinder-hemisphere structure ($L/D=0.5$, $h/D=0.01$, $E=1.0$, $\nu=0.2$, $\rho=1.0$, $L=100$) for $m=1$

n	FEM	Series solution*	FEM**	VFD***	Numerical integration****
0	2.0590	2.0584	2.0589	2.0589	2.0597
1	0.9433	0.9431	0.9438	0.9435	0.5436
2	1.6212	1.6091	1.6205	1.6222	1.6207
3	1.3081	1.3057	1.3070	1.3100	—
4	1.0952	1.0942	1.0940	1.0978	—

Natural frequencies *, **, ***, and **** are taken from ref. 14.
*** Variational finite difference method.
**** Runge-Kutta integration method.

Table 3 Natural frequences of a hyperbolic shell
$a=25.6032$m $b=63.9064$m
(a and b are parameters in the equation of a hyperbola)
$t_z=18.5928$m (height between the troat and the top)
$b_z=82.1944$m (height between the throat and the base)
$h=0.127$m $E=2.0684\times10^{10}$N/m^2 $\rho=2.4046\times10^3$kg/m^3 $\nu=0.15$

n	m	FEM	FEM*	Theor.**	FDM***	FEM****
0	1	—	6.2329	—	—	—
	2	7.7488	7.7521	7.7525	8.1500	—
	3	11.4196	11.4290	11.4213	11.3799	—
1	1	3.2885	3.2897	3.2897	3.3345	—
	2	6.7922	6.7933	6.7932	6.8816	—
	3	10.5228	10.5230	10.5250	10.5316	—
2	1	1.7662	1.7664	1.7661	1.7848	1.7718
	2	3.6898	3.6893	3.6946	3.7234	3.6954
	3	6.9592	6.9556	6.9590	6.9553	—
3	1	1.3764	1.3759	1.3755	1.3927	1.3883
	2	1.9947	1.9935	1.9912	2.0150	1.9947
	3	4.3416	4.3370	4.3272	4.3353	—
4	2	1.1822	1.1812	1.1812	1.2003	1.1827
	2	1.4497	1.4479	1.4481	1.4597	1.4645
	3	2.7828	2.7779	2.7788	2.7762	2.7895
5	2	1.0346	1.0335	1.0352	1.0441	1.0413
	3	1.4319	1.4295	1.4299	1.4417	1.4417
	1	2.0621	2.0570	2.0568	2.0555	2.0668
6	2	1.1491	1.1481	1.1472	1.1544	1.1586
	3	1.3278	1.3259	1.3236	1.3335	1.3334
	2	2.0215	2.0155	2.0149	2.0152	2.4979
7	3	1.3042	1.3032	1.3020	1.3055	—
	3	1.5164	1.5148	1.5140	1.5189	—
	4	1.9293	1.9234	1.9225	1.9200	—

Natural frequencies *, **, ***, and **** are taken from ref. 15.
* Ring element having 24 degrees of freedom was used.
** Theoretical results were obtained by solving the differential equations of motion.
*** Finite difference method. **** Doubly-curved element was used.

by the factor $(100/D)$ (E/ρ), provided that they have same $\nu=0.2$.

Third example is a free vibration of a shell having arbitrary shape of revolution like cooling tower (Fig. 3). Cooling tower shell is assumed to be a hyperbolic shell, and the top edges are free and the bottom edges are clamped. Natural frequencies are calculated and compared with other results in Table 3. Deb Nath (ref. 15) obtained the natural frequencies by using a ring element having 24 degrees of freedom in which dispacements u, v, and w maintain continuity up to the third derivatives across interelement boundaries. In Table 3, natural frequencies denoted by Theor.** were obtained analytically solving the differential equations of motion, and FDM*** is the results by finite difference-method. Also the results FEM**** were obtained by using doubly-curved shell element by Deb Nath (ref. 15). All referred frequencies are taken from ref. 15, and the frequencies in Table 3 are in good agreement with each other.

When a shell is rotating, natural frequencies are calculated for the shell in the first example with the same boundary conditions. The results when Ω is 3,600rpm are compared with theoretical frequencies(ref. 16) in Table 4. In Fig. 4, natural frequencies vs. rotating speed Ω for various n and m are given.

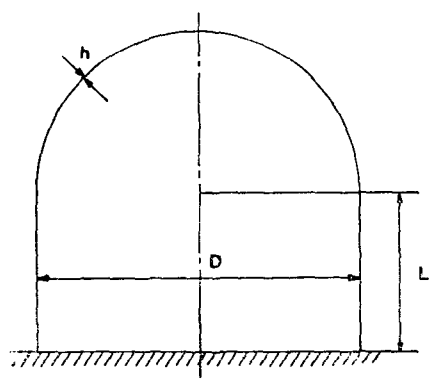

Fig. 2 Cylinder-hemisphere shell clamped at its base ($L/D=0.5$, $h/D=0.01$, $E=1.0$, $\nu=0.2$, $\rho=1.0$, $L=100$)

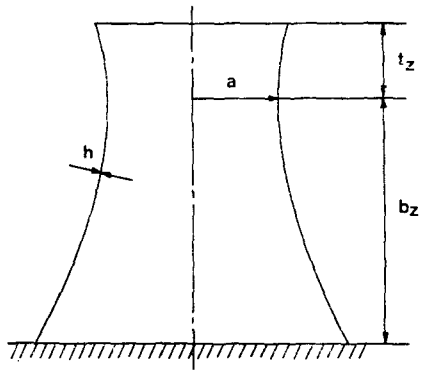

Fig. 3 Hyperbolic shell with free-clamped ends
$a=25.6032$m $b=63.9064$m
(a, b are parameters in the equation of a hyperbola)
$t_z=18.5928$m $b_z=82.1944$m
$h=0.127$m $E=2.0684\times10^{10}$N/m^2
$\rho=2.4046\times10^3$kg/m^3 $\nu=0.15$

These results show clearly the presence of traveling waves in rotating shell. In case of rotating, two frequencies, forward and backward frequencies are obtained for each circumferential wave number and meridional mode number. The results in Table 4 are well consistent with each other, while maximum difference between them is about 7% when $n=1$.

6. Conclusions

A vibration analysis of rotating thin shell by finite element method is presented. Natural frequencies of any rotating axi-symmetric shell can be obtained. Not only the conical frustrum type element having to nodes used here, but also any other shell elements can be incorporated with the presented FEM formulation. Although the effects of rotation on the eigenvalues is of main concern in this paper, the solution procedure can be used to obtain the eigenvalues of stationary shell which have many applications in engineering like cooling

Table 4 Natural frequencies when Ω=3600rpm for a clamped=free cylindrical shell of radius=63.5mm, length=502mm, thickness=1.63mm, $E=2.1\times10^{11}N/m^2$, $\nu=0.28$, $\rho=7.8\times10^3kg/m^3$(Hz)

n		m=1		m=2		m=3	
1	FEM	410.9	527.8	2,001	2,108	4,352	4,462
	Theory*	441.9	558.4	2.442	2,550	5,020	5,132
2	FEM	276.5	372.2	904.0	998.7	2,180	2.274
	Theory	280.0	375.6	975.1	1,070	2,353	2,447
3	FEM	745.5	817.5	896.1	968.1	1,456	1.528
	Theory	747.4	819.3	905.8	977.8	1,486	1,558
4	FEM	1,500	1,506	1,507	1,564	1,714	1,771
	Theory	1,453	1,509	1,511	1,568	1,715	1,772
5	FEM	2,355	2,401	2,396	2,442	2,504	2,551
	Theory	2,360	2,406	2,402	2,448	2,505	2,552
6	FEM	3,461	3,500	3,497	3,536	3,578	3,617
	Theory	3,467	3,506	3,506	3,545	3,583	3,622

* Theoretical frequencies are taken from ref. (16).

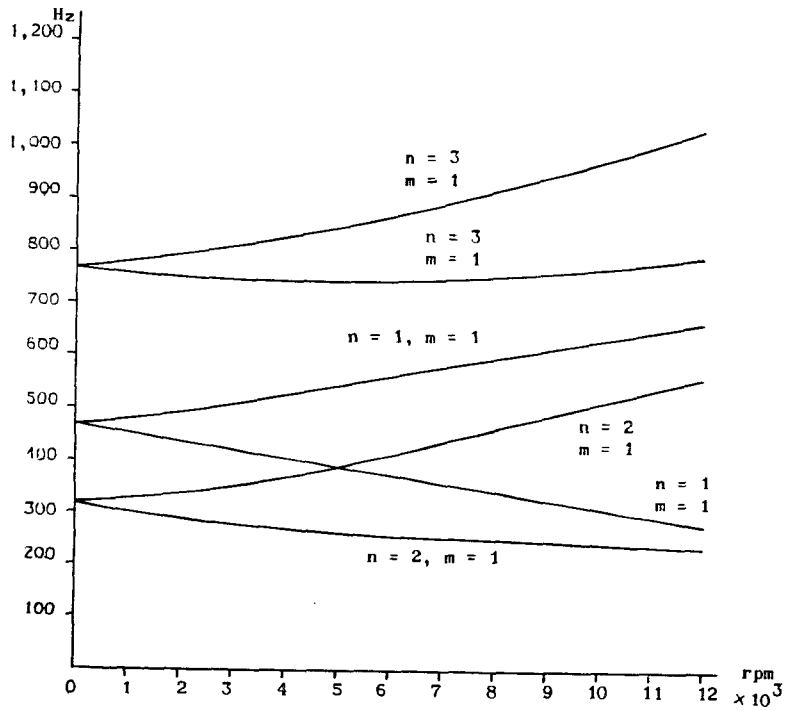

Fig. 4 Natural frequencies vs. rotating speed Ω for a clamped-free cylindrical shell of radius=63.5mm, length=502mm, thickness=1.63mm, $E=2.1\times10^{11}N/m^2$, $\nu=0.28$, $\rho=7.8\times10^3kg/m^3$

tower, containment building in nuclear power plant, and heat exchangers, etc., by simply setting $\Omega=0$. The comparisons between the results by present FEM analysis and the results by various methods such as analytic method, numerical integration method, and FEM using

different elements or shape functions show a very good correspondence.

As degrees of freedom are reduced by expanding the circumferential variables into Fourier series, the number of equations to be solved is greatly reduced which results in a considerable saving of computing time. The solution procedures of extracting eigenvalues can be used to solve the eigenvalue problems of the small banded-large order matrix containing skew-symmetric Coriolis matrix.

References

(1) H. J. Macke, Traveling-Wave Vibration of Gas Turbine Engine Shells, Journal of Engineering for Power, Vol. 88, No. 2, pp. 179~187, 1966

(2) A.V. Srinivasan and G.F. Lauterbach, Traveling Waves in Rotating Cylindrical Shells, Journal of Engineering for Industry, Vol. 93, No. 4, pp. 1229~1231, 1971

(3) L.E. Penzes and H. Kraus, Free Vibration of Prestressed Cylindrical Shells having Arbitrary Homogeneous Boundary Conditions, AIAA, Vol. 10, No. 10, pp. 1309~1313, 1972

(4) J. Padovan, Natural Frequencies of Rotating Prestressed Cylinders, Journal of Sound and Vibration, Vol. 31, pp. 469~482, 1973

(5) J. Padovan, Traveling Waves Vibrations and Buckling of Rotating Anisotropic Shells of Revolution by Finite Elements, Int. Journal of Solids & Structures, Vol. 11, pp. 1367~1380, 1975

(6) H. Radwan and J. Genin, Non-Linear Modal Equations for Thin Elastic Shells, Int. J. Non-Linear Mechanics, Vol. 10, pp. 15~29, 1975

(7) K.J. Bathe, Finite, Element Procedures in Engineering Analysis, Chap. 11, Prentice-Hall, New Jersey, 1982

(8) K.K. Gupta, On a Combined Strum Sequence and Inverse Iteration Technique for Eigenproblem Solution of Spinning Structures, Int. Journal for Numerical Methods in Engineering, Vol. 7, pp. 509~518, 1973

(9) K.K. Gupta, Free Vibration Analysis of Spinning Structural Systems, Int. Journal for Numerical Methods in Engineering, Vol. 5, pp. 395~418, 1973

(10) W.H. Wittrick and F.W. Williams, On the Free Vibration Analysis of Spinning Structures by Using Distributed Mass Models, Journal of Sound and Vibration, Vol. 82, No. 1, pp. 1~15, 1982

(11) K.J. Bathe, E.L. Wilson and F.E. Peterson, SAP5-A Structural Analysis Program for Static and Dynamic Response of Linear System, 1974

(12) C.B. Sharma, Calculation of Natural Frequencies of Fixed-Free Circular Cylindrical Shells, Journal of Sound and Vibration, Vol. 35, No. 1, pp. 55~76, 1974

(13) P.A.T. Gill, Vibration of Clamped-Free Circular Cylindrical Shells, Journal of Sound and Vibration, Vol. 25, pp. 501~502, 1972

(14) G.D. Galletly and J. Mistry, The Free Vibration of Cylindrical Shells with Various End Closures, Nuclear Engineering and Design, Vol. 30, pp. 249~268, 1974

(15) J.M. Deb Nath, Free Vibration, Stability and "Non-Classical Modes" of Cooling Tower Shells, Journal of Sound and Vibration, Vol. 33, No. 1, pp. 79~101, 1974

(16) H.S. Kim, Vibration Characteristics of Rotating Cylindrical Shells, M.S. Thesis, KAIST, 1982